



ELSEVIER

Thermochimica Acta 286 (1996) 1–15

thermochimica
acta

Thermoanalytical study of benzimidazole complexes with transition metal ions: Copper (II) complexes

S. Materazzi*, R. Curini, G. D'Ascenzo,

Department of Chemistry, University "La Sapienza", p.le A. Moro 5, 00185, Rome, Italy

Received 9 February 1996; accepted 21 March 1996

Abstract

The benzimidazole molecule (Benz) is known to play a fundamental role in many biological systems; it is moreover, extensively used in industrial processes as a corrosion inhibitor for metal and alloy surfaces.

The synthesis and the thermal profile of some Cu (II) complexes of benzimidazole of general formula $\text{CuBenz}_4\text{X}_2$ are proposed.

A parallel study of these complexes with an ionization mass spectrometer is also reported.

Keywords: Copper(II) complexes; Benzimidazole; TG-FTIR; DSC; Ionization mass spectroscopy

1. Introduction

The coordination chemistry of azoles acting as ligands in copper compounds has been studied in the context of modeling biological systems. Cu(II)-imidazole bonding has been observed in the histidine-containing plastocyanin [1] and azurin peptides [2]. Extensive studies of the electronic spectra of $(\text{CuImidazole}_4)^{2+}$ and closely related substituted imidazole complexes have aided the characterization of these peptide systems [3–6]. Moreover, azoles such as benzotriazole, and benzimidazole are extensively used in industrial processes as corrosion inhibitors for metal and alloy surfaces, particularly that of copper [6–10]. The nature of the passivating film on copper has

* Corresponding author.

been studied by a variety of experimental techniques including infrared spectroscopy [9–10], X-ray photoelectron spectroscopy [11–15], and ellipsometry [16].

Many authors have prepared complexes of benzimidazole (Benz) with transition metal ions such as Co(II), Ni(II), Cu(II), and although many studies of crystal structure can be found in the literature [17–19], there are few studies of the thermal stability and decomposition steps of these complexes [20]. Moreover, unusual behaviors of these complexes (supposed isomers) have been explained by thermal investigations [21,22], the results show that Ni(II) forms dimeric complexes with benzimidazole of formula $[\text{Ni}_2\text{Benz}_8\text{X}_3] \text{X}$ where X is Cl^- or Br^- , and the dimeric structure changes to the monomeric one by means of a temperature-induced anation reaction.

In this work, a thermal profile of some Cu(II) complexes of benzimidazole of general formula $\text{CuBenz}_4\text{X}_2$, with $\text{X} = \text{Cl}^-$, Br^- , NO_3^- , ClO_4^- or SO_4^{2-} , is proposed by means of thermogravimetric (TG) analysis, coupled thermogravimetry–FTIR analysis (TG–FTIR) and differential scanning calorimetry (DSC).

A parallel qualitative study of these complexes with a ionization mass spectrometer is also reported.

2. Experimental

2.1. Materials

Benzimidazole and the Cu(II) salts were purchased from Aldrich Chemical Co. The solvents were all of the highest purity available.

2.2. Synthesis of the complexes

Cu(II) complexes were first prepared as described by Goodgame and Haines [23]. The TG and DSC analysis of these compounds show a tendency of these complexes to ontrap ligand molecules because of the high speed of complex formation and precipitation, and the ligand molecules were not strongly bonded. So, as for the synthesis of the $\text{NiBenz}_4\text{Cl}_2$ and $\text{NiBenz}_4\text{Br}_2$ complexes [21, 22], the metal solution was slowly added, with stirring, to the ligand solutions (both solutions were 10^{-2} M in stoichiometric ratio), and the final solution was refluxed for some hours. The complexes so obtained show the right metal/ligand ratio and, if possible, the presence of water molecules in the structure. Often the metal/ligand ratio was lowered to prevent the tendency to co-precipitation.

2.3. Instrumental

Thermoanalytical curves were obtained using a Perkin–Elmer DSC 7. The atmosphere was oxygen, nitrogen, or air, with a flow rate of $50\text{--}100 \text{ ml min}^{-1}$. The heating rate was ranged between 5 and $40^\circ\text{C min}^{-1}$. The thermobalance was coupled with a Perkin–Elmer FTIR, model 1760X, to obtain the infrared spectra of gases evolved during the thermogravimetric analysis. The TGA 7 is coupled to the heated gas cell of

the FTIR instrument by means of a heated transfer line. Gaseous or vaporized components are flushed by the suitable gas and the temperatures of the cell and of the transfer line are independently selected. The only materials in contact with the sample gases are PTFE of the transfer line, KBr of the cell windows and the glass of the TGA/7 furnace.

The mass spectra were obtained with a Perkin–Elmer API1 (atmospheric pressure ionization) mass spectrometer. The complexes were dissolved in absolute ethanol, absolute methanol, or acetonitrile to give 10^{-2} g L⁻¹ solutions.

3. Results

The Complexes obtained were all of general formula $\text{CuBenz}_4\text{X}_2$.

3.1. $\text{CuBenz}_4\text{Cl}_2 \cdot 3\text{H}_2\text{O}$ (blue)

The TG and DTG curves (Fig. 1a) show four main steps corresponding to the loss of three molecules of water, then to the sublimation of two benzimidazole molecules, and finally to the decomposition to give the metal oxide. In the DSC curve (Fig. 1b) the first endothermic process appears due to the loss of H₂O, and is followed by an exothermic one. At 200°C an endo–exothermic peak is present, due to the dimeric → monomeric transition. The following endothermic process corresponds to the sublimation of two benzimidazole molecules, and around 350°C the decomposition starts, giving CuO.

3.2. $\text{CuBenz}_4\text{Br}_2 \cdot 2\text{H}_2\text{O}$ (grey)

The TG and DTG curves (Fig. 2a) show a first process, the loss of two molecules of water, and then two main processes: the first of these is the superimposition of at least three processes, and the second shows two overlapped processes to give the copper oxide. The DSC curve (Fig. 2b) shows two endothermic processes separated by an exothermic peak. At 175°C, as for the $\text{CuBenz}_4\text{Cl}_2$ complex, an endo–exothermic peak is present because of the dimeric → monomeric change. The following processes correspond to the sublimation and then to the decomposition reactions.

3.3. $\text{CuBenz}_4(\text{NO}_3)_2$ (violet)

This complex decomposes in three well defined steps, as can be seen from TG and DTG curves (Fig. 3a). The DSC curve (Fig. 3b) shows an exothermic peak at 230°C and then two exothermic processes, the first at 360°C is immediately followed by the second, giving CuO.

3.4. $\text{CuBenz}_4(\text{SO}_4) \cdot \text{H}_2\text{O}$ (violet)

The TG and DTG curves (Fig. 4a) show a first step for the loss of one water molecule, followed by a second step due to the loss of benzimidazole and then two

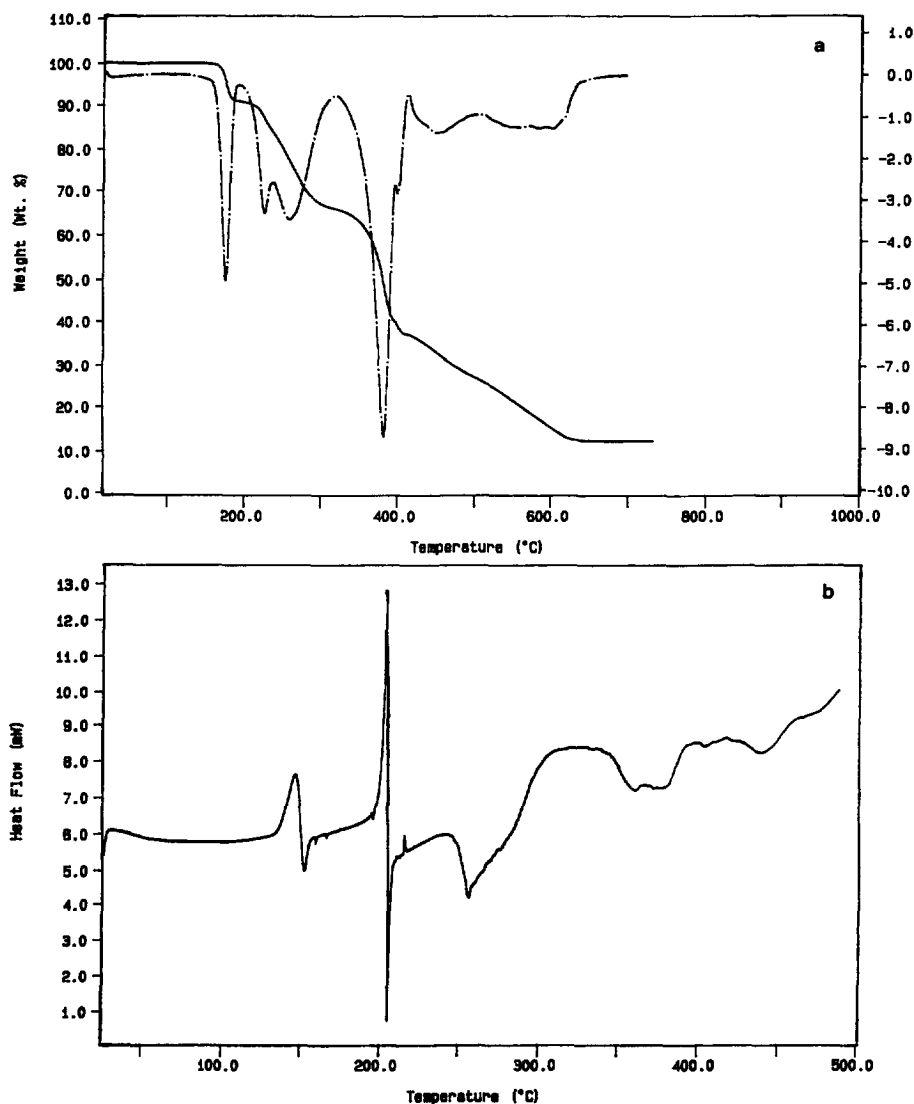


Fig. 1. $\text{CuBenz}_4\text{Cl}_2 \cdot 3\text{H}_2\text{O}$: (a) — TG curve, --- DTG curve; (b) — DSC curve; scanning rate: $10^{\circ}\text{C min}^{-1}$, air flow $50\text{--}100 \text{ ml min}^{-1}$.

poorly resolved processes resulting in the formation of the metal oxide. The DSC curve (Fig. 4b) shows a first endothermic peak related to the water loss and then a second process that is the result of an endothermic peak due to the sublimation and of an exothermic peak due to the decomposition of the benzimidazole; the decomposition to CuO follows.

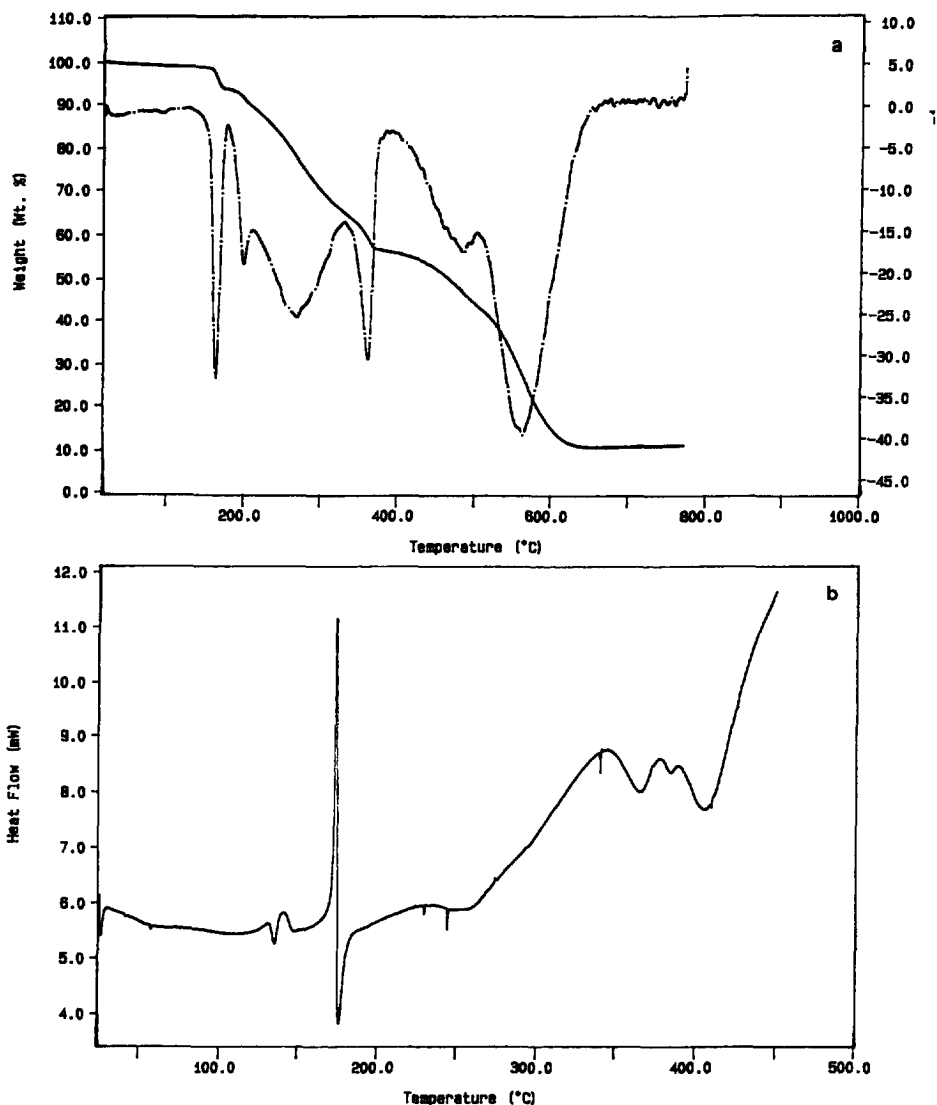


Fig. 2. $\text{CuBenz}_4\text{Br}_2 \cdot 2\text{H}_2\text{O}$: (a) — TG curve, --- DTG curve; (b) — DSC curve; scanning rate: $10^\circ\text{C min}^{-1}$; air flow $50\text{--}100\text{ mL min}^{-1}$.

3.5. $\text{CuBenz}_4(\text{ClO}_4)_2(\text{lilac})$

Three processes appear in the TG and DTG curves (Fig. 5a), and the corresponding DSC curve (Fig. 5b) shows a sharp process at 271°C followed by two exothermic processes to give the metal oxide.

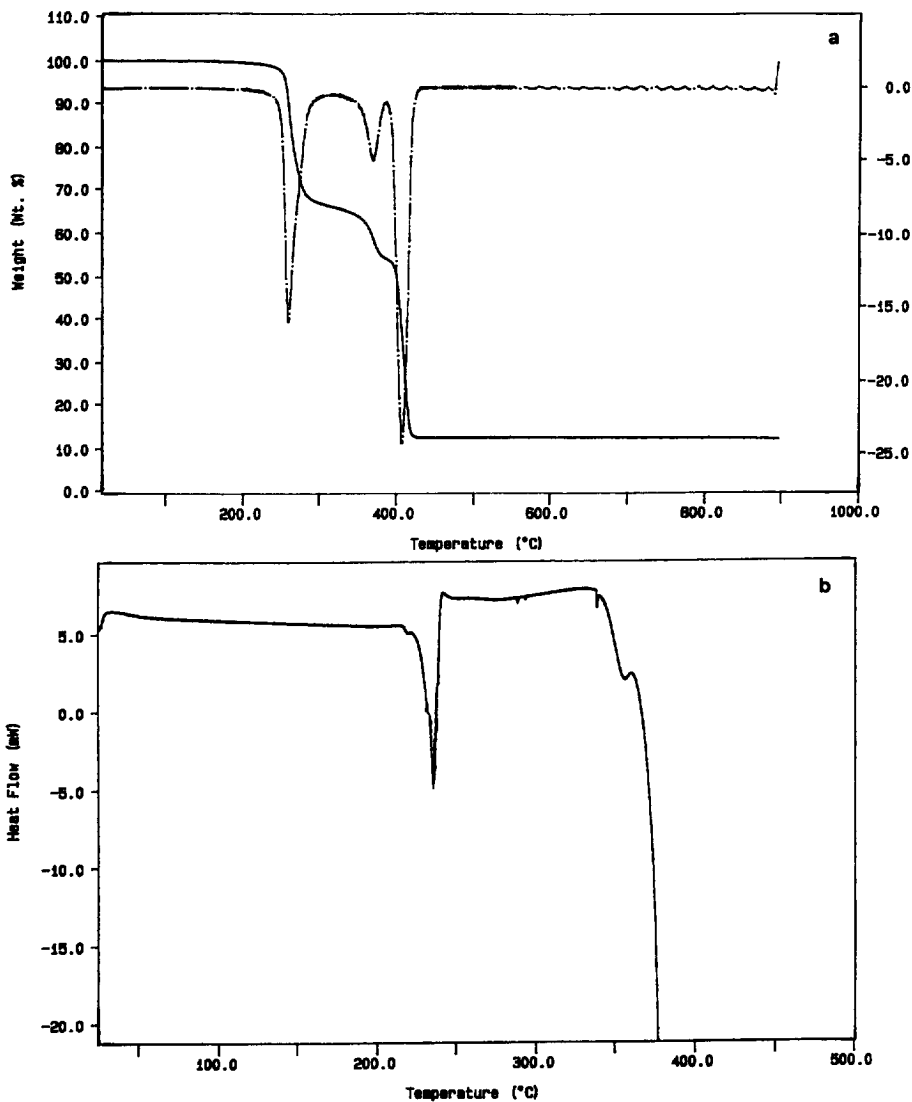


Fig. 3. $\text{CuBenz}_4(\text{NO}_3)_2$: (a) — TG curve, --- DTG curve; (b) — DSC curve; scanning rate: $10^\circ\text{C min}^{-1}$; air flow $50\text{--}100\text{ mL min}^{-1}$.

3.6. $\text{CuBenz}_2(\text{red})$

This complex (“inner complex”) shows only one TG process (Fig. 6a) in which it decomposes exothermically. The DSC curve (Fig. 6b) shows only one exothermic peak at 370°C . The same complex has been examined in previous work [20].

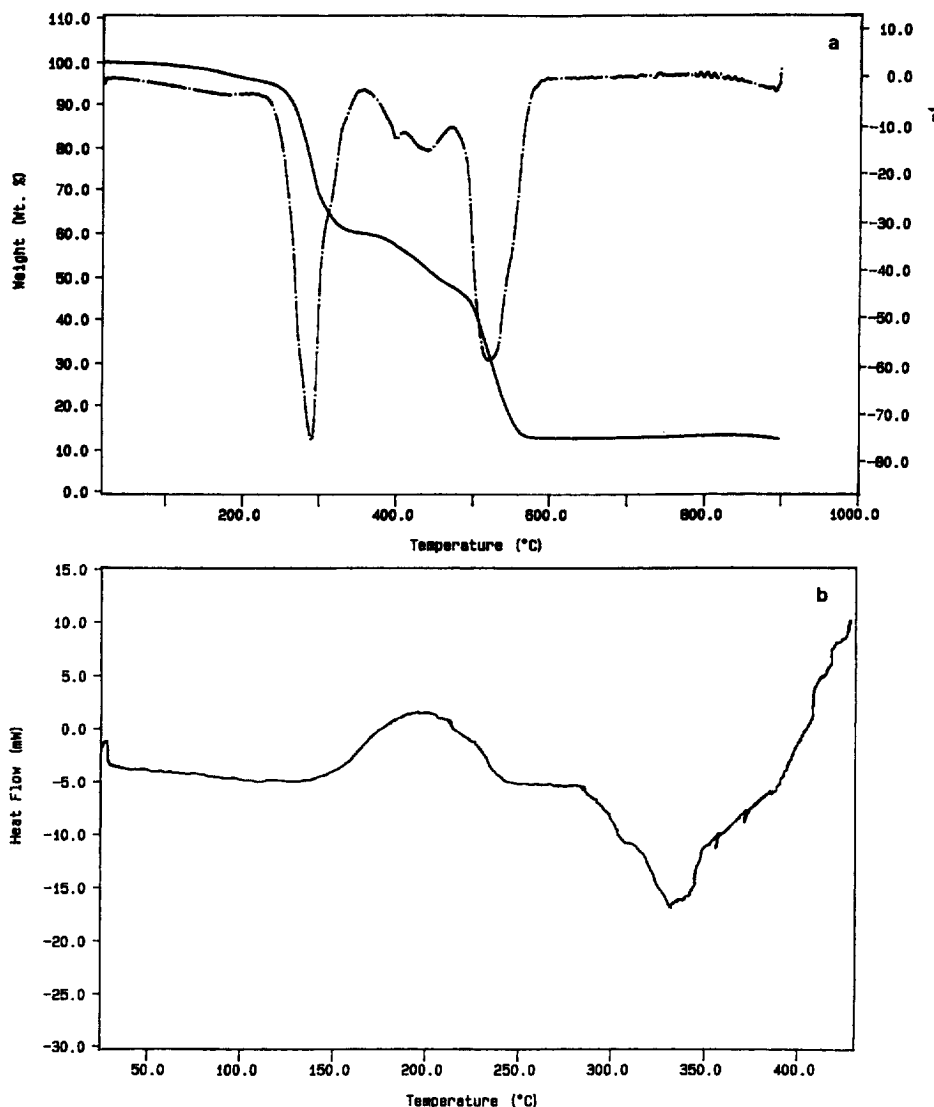


Fig. 4. $\text{CuBenz}_4\text{SO}_4$: (a) — TG curve, --- DTG curve; (b) — DSC curve; scanning rate: $10^{\circ}\text{C min}^{-1}$; air flow 50–100 mL min^{-1} .

4. Discussion

Benzimidazole is a ligand molecule that can form complexes with the Cu(II) ion of the type $\text{CuBenz}_4\text{X}_2$; complexes of this stoichiometry were formed when solutions of benzimidazole in organic solvents were added to solutions of Cu(II) salts, even when the metal/ligand ratio was less than 1:4; this contrasts with the behavior of pyridine or other unidentate heterocyclic ligands.

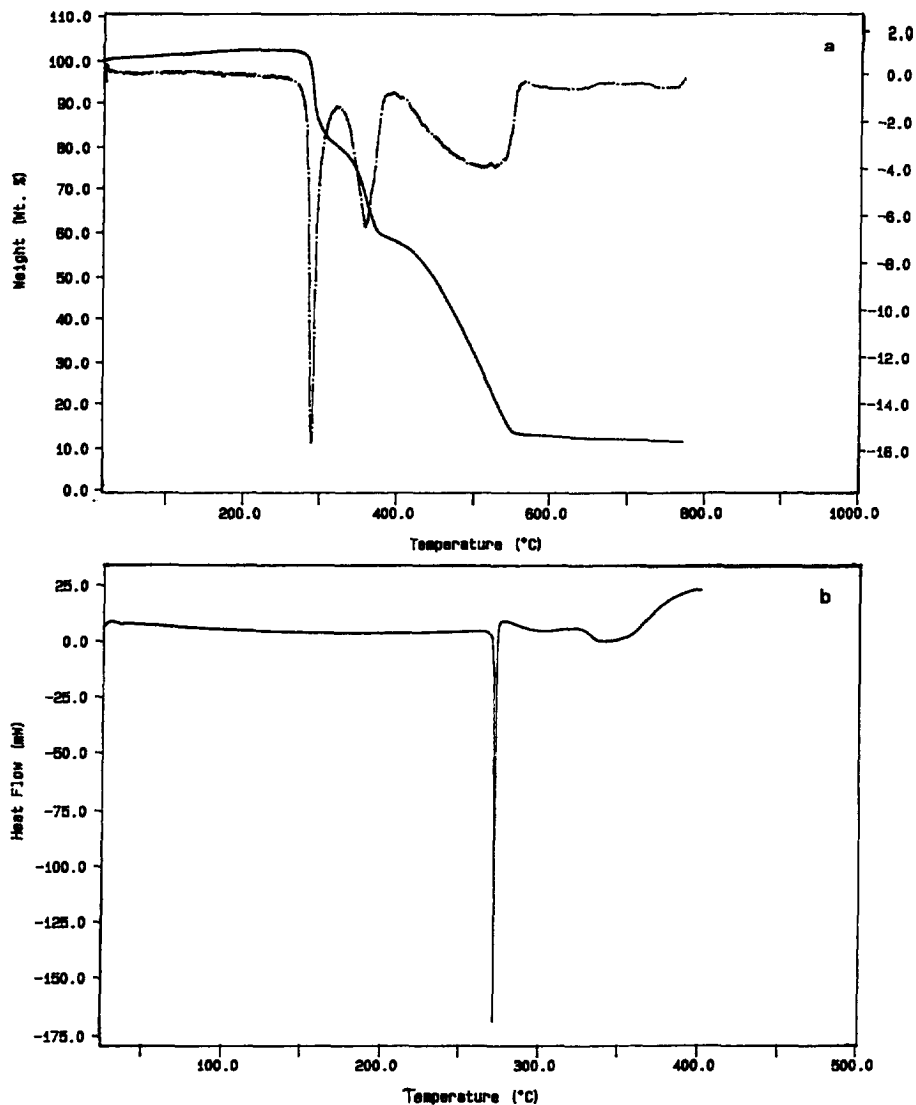


Fig. 5. $\text{CuBenz}_4(\text{ClO}_4)_2$ (a) — TG curve, --- DTG curve; (b) — DSC curve; scanning rate: $10^{\circ}\text{C min}^{-1}$; oxygen flow $50\text{--}100\text{ mL min}^{-1}$.

As also reported by Goodgame and Haines [23], the reflectance spectra are of the type generally found for tetragonally distorted octahedral complexes, with the four ligand molecules in the xy plane and the anions on, or close to, the z axis. The benzimidazole molecules are forced, for steric reasons, to lie with their molecular planes at an angle to the CuN_4 plane. There will therefore be some steric hindrance to the approach of larger anions; moreover, the absence of water molecules in complexes with large anions is also observed.

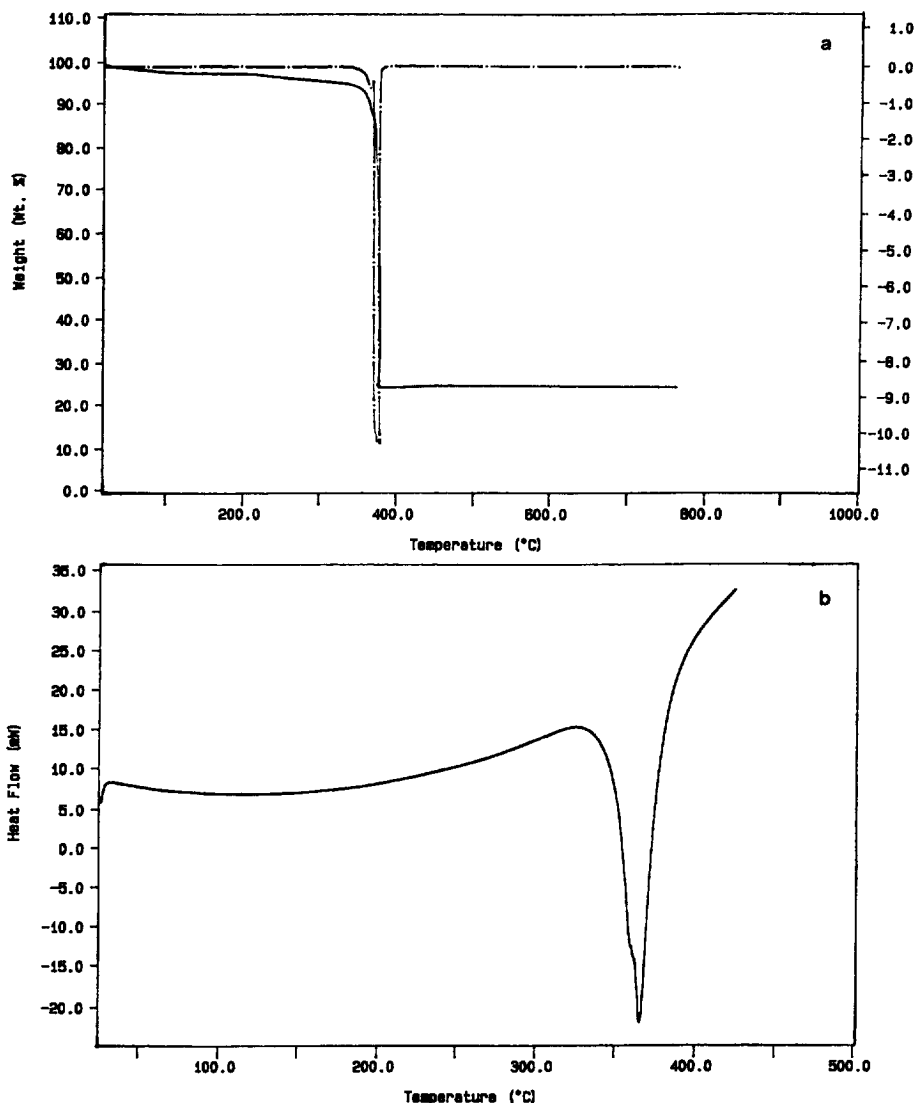


Fig. 6. CuBenz₂: (a) — TG curve, --- DTG curve; (b) — DSC curve; scanning rate: 10 °C min⁻¹; oxygen flow 50–100 mL min⁻¹.

The TG–FTIR spectra show that the solvent lost in the first TG step from the complexes with SO₄²⁻, Cl⁻ and Br⁻ anions is water (Fig. 7a). The successive sublimation process can be inhibited if an oxygen flow is used during the analysis; with time, moreover, the complex gets older and only with O₂ flow does the correct decomposition occur; with air or nitrogen flow sublimation of the benzimidazole involves part of the complex, so lowering the final oxide percent. The TG–FTIR spectra related to the

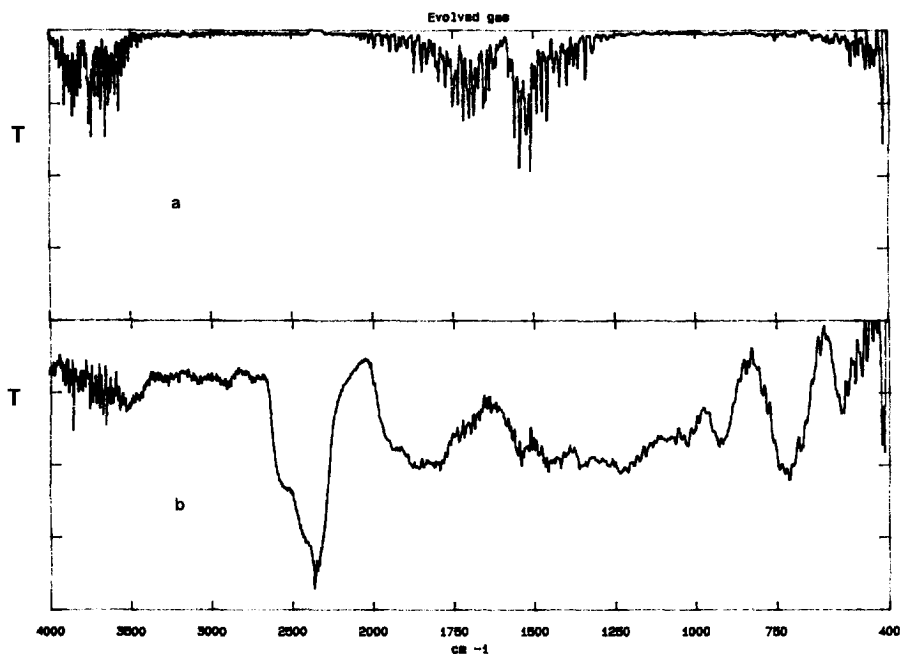


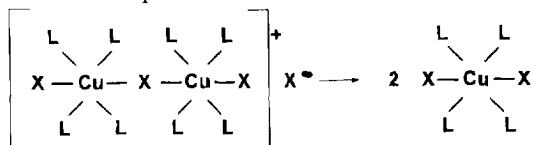
Fig. 7. TG-FTIR spectra: infrared spectra of the gas evolved during the TG steps; resolution: 4 cm^{-1} .

loss of the first two benzimidazole molecules, with oxygen flow, show the characteristic bands for the decomposition of standard benzimidazole (Fig. 7b).

On aging, the complexes show different behavior:

1. The $\text{CuBenz}_4\text{Cl}_2$ complex does not lose water molecules but, despite the oxygen flow, sublimation occurs in the same way, changing the final oxide percent; the decomposition is shifted to lower temperatures;
2. The $\text{CuBenz}_4\text{Br}_2$ complex loses one water molecule after 14 days, but the decomposition range does not change; after 23 days, the amount of solvent decreases and the last decomposition process is shifted to lower temperatures;
3. The $\text{CuBenz}_4(\text{NO}_3)_2$ complex does not change with time;
4. The $\text{CuBenz}_4\text{SO}_4$ complex loses the water molecule on aging, and the final CuO residue changes probably because the external surface of the complex agglomerate changes to oxide, highering the CuO percent of the final plateau of the TG scan;
5. The $\text{CuBenz}_4(\text{ClO}_4)_2$ complex shows a lowering of the temperature for the last decomposition process to give CuO with a lower complex stability; and
6. The CuBenz_2 complex ("inner complex") does not change with time.

The Cl^- and Br^- complexes have a dimeric structure as for the corresponding Ni(II) complexes: from the DSC curves and endo-exothermic peak can be noted, after the loss of the solvent, due to the temperature-induced reaction



(L = benzimidazole X = Cl or Br).

By DSC, we obtained either the dimeric unsolvated complexes or the monomeric unsolvated complexes respectively, by heating the original complexes, either after the peak of the solvent loss or after the endo–exothermic peak. While the desolvation does not imply thermal changes to the decomposition behavior, the monomeric complexes show a different thermal profile with a higher thermal stability in the last decomposition process (Fig. 8).

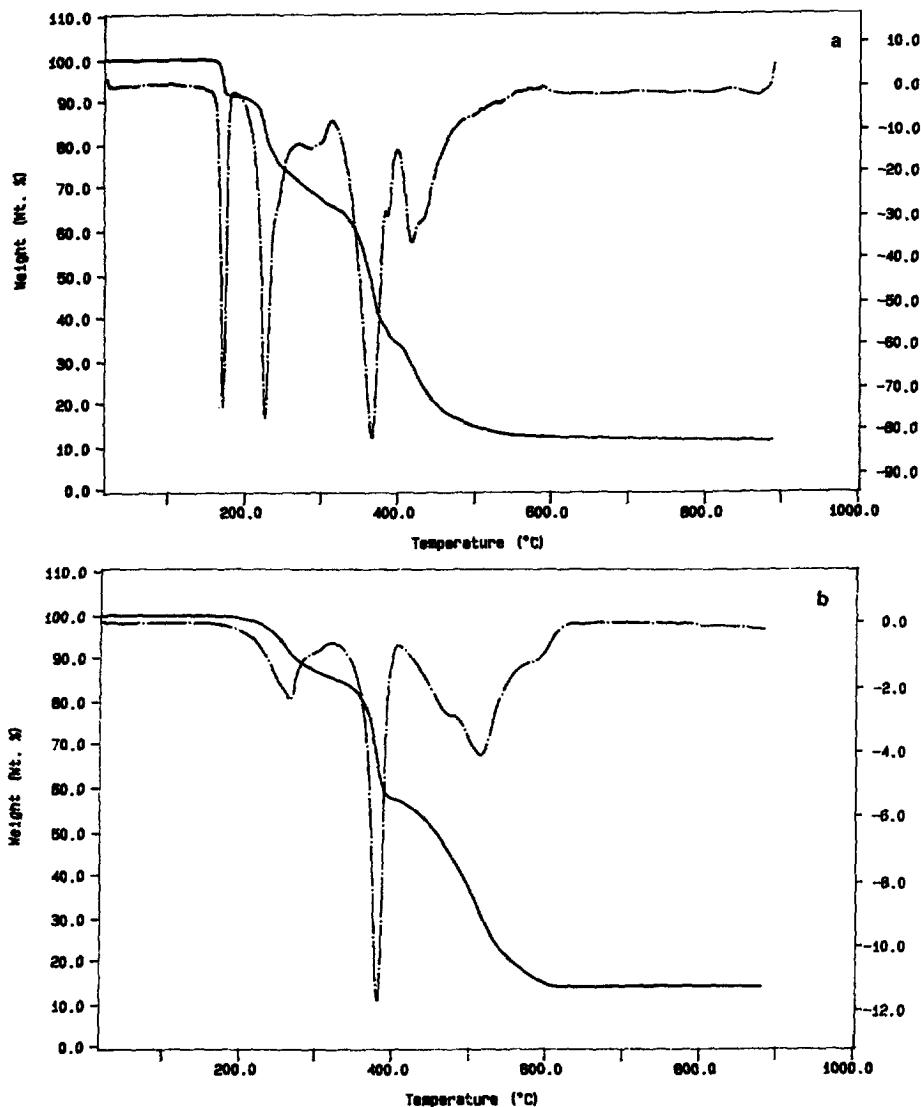
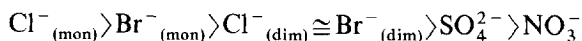


Fig. 8. (a) $\text{CuBenz}_4\text{Cl}_2 \cdot 3\text{H}_2\text{O}$ (dimeric): (a) — TG curve, --- DTG curve; (b) $\text{CuBenz}_4\text{Cl}_2$ (monomeric): — TG curve, --- DTG curve; scanning rate: $10^\circ\text{C min}^{-1}$; oxygen flow $50\text{--}100\text{ mL min}^{-1}$.

A thermal stability scale can be proposed:



Looking at the DSC curves, the process due to the loss of the two benzimidazole molecules (after the endo–exothermic peak for the Cl^- and Br^- complexes) overlaps the process due to the anation reaction. The ΔH values for the reaction $\text{CuBenz}_4\text{X}_2 \rightarrow \text{CuBenz}_2\text{X}_2 + 2\text{Benz}$ has been calculated and decreases in the order $\text{Cl}^- > \text{Br}^- > \text{NO}_3^- > \text{SO}_4^{2-}$ (see Table 1). All the processes are exothermic except that for the SO_4^{2-} complex which is endothermic; this is probably because of the different structural position of the sulfate anion.

The ClO_4^- complex shows a sharp exothermic DSC process with a higher ΔH value; this is due to the exothermic decomposition of the same anion; the TG curve confirms the different decomposition behavior of this complex (if compared with all the other complexes) with two well defined steps followed by the final decomposition to give CuO . A parallel study has been carried out by a ionization mass spectromere. Fig. 9 shows the mass spectra of the complexes, when absolute ethanol is used as flow solvent. The fragments common to all the five complexes correspond to the $(\text{CuBenz}_4)^{2+}$ ion ($m/z = 268$) and to the $(\text{CuBenz}_2)^+$ ion ($m/z = 299$); only for the nitrate complex is the relative intensity the same for the two peaks; for all the other complexes the m/z 268 peak is of lower intensity.

In the sulfate complex spectrum the $(\text{CuBenz}_4)^{2+}$ peak is of very low intensity because of the low binding energy of the fourth ligand molecule.

The peak of the $(\text{CuBenz}_3)^{2+}$ ion ($m/z = 209$) is not present in the ClO_4^- complex spectrum, so we can suppose that two ligand molecules have a similar binding energy and the m/z 209 peak has a low formation probability. The peak at m/z 344 can be attributed to the $(\text{CuBenz}_2 \cdot \text{EtOH})^+$ ion, being present only in the anhydrous complexes.

The Cl^- , Br^- and SO_4^{2-} complexes (hydrated) show a peak at m/z 355, probably due to the $(\text{CuBenz}_2 \cdot 3\text{H}_2\text{O})^+$ ion.

Only the nitrate complex shows the $(\text{CuBenz}_2\text{X})^+$ ion ($m/z = 361$), probably because of the higher metal–ion interaction of the Cu^{2+} with the NO_3^- in organic solution.

When methanol was used as flow solvent, similar mass spectra were obtained, with no increase in the sizes of the characteristic peaks. The same results were obtained when using acetonitrile as flow solvent.

Table 1
 ΔH values for the anation-reaction of each complex

Complex	$\Delta H/(\text{J/g}^{-1})$
$\text{CuBenz}_4\text{Cl}_2$	– 1034 Jg
$\text{CuBenz}_4\text{Br}_2$	– 180 Jg
$\text{CuBenz}_4(\text{NO}_3)_2$	– 148 Jg
$\text{CuBenz}_4\text{SO}_4$	+ 141 Jg
$\text{CuBenz}_4(\text{ClO}_4)_2$ (decomp.)	– 2767 Jg

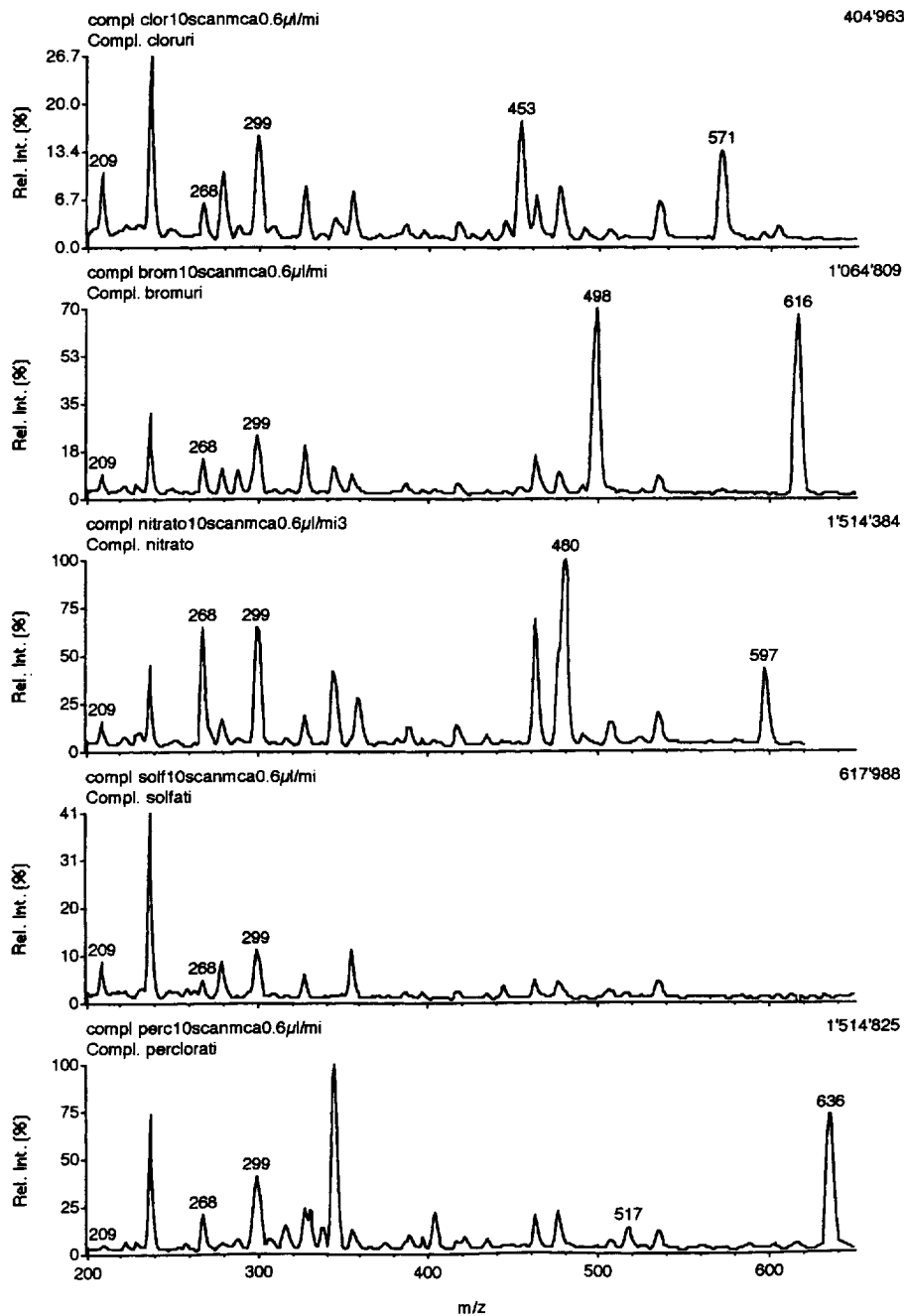


Fig. 9. Mass spectra of the complexes: (a) CuBenz₄Cl₂; (b) CuBenz₄Br₂; (c) CuBenz₄(NO₃)₂; (d) CuBenz₄SO₄; (e) CuBenz₄(ClO₄)₂.

Table 2
m/z values for each complex

Ions	Peak (<i>m/z</i>)				
	Cl ⁻	Br ⁻	NO ₃ ⁻	ClO ₄ ⁻	SO ₄ ²⁻
(CuBenz ₄) ²⁺	268	268	268	268	268
(CuBenz ₃) ²⁻	209	209	209	209	209
(CuBenz ₂) ⁺	299	299	299	299	299
(CuBenz ₄ X) ⁺	571	616	597	636	–
(CuBenz ² X) ⁺	453	498	480	571	–
(CuBenz ₂ X) ⁻	335	379	361	399	–

Though no solubility differences among the three solvents were found, saturated ethanolic solutions of the Cl⁻ and Br⁻ complexes were prepared and injected to demonstrate the presence of the dimeric complexes in organic solvents; no peaks were found at *m/z* 1178, related to the (Cu₂Benz₈Cl₃)⁺ ion, or at *m/z* 1311, related to the (Cu₂Benz₈Br₃)⁺ ion.

The experimental *m/z* values and the corresponding proposed ions are summarized in Table 2.

5. Conclusions

The benzimidazole complexes of divalent copper show different thermal behavior on changing the anion. As for the Ni(II) complexes, only the Cl⁻ and the Br⁻ complexes are of dimeric structure; with larger anions, only the monomeric form is possible for steric reasons and this is also proved by the absence of water molecules in the crystalline structure. The presence of one water molecule in the CuBenz₄SO₄ complex structure is possible because of the different spatial disposition of the SO₄²⁻ anion. With time the complexes show a tendency to become thermochemically less stable.

The parallel study with ionization mass spectroscopy gave evidence for the dimeric complexes in aqueous solvents.

Acknowledgment

This work was aided by research grants from Ministry of University and Scientific and Technologic Research (MURST, Italy).

References

- [1] P.M. Coleman, H.C. Freeman and J.M. Guss, *Nature* (London), 272 (1980) 319.
- [2] E.T. Adman, R.E. Steinkamp and L.C. Sicker, *J. Mol. Biol.*, 123 (1978) 35.
- [3] T.G. Fawcett, E.E. Bernarducci and H.J. Schugar, *J. Am. Chem. Soc.*, 102 (1980) 2598.

- [4] E.E. Bernarducci, W.F. Schwingdinger and H.J. Schugar, *J. Am. Chem. Soc.*, 103 (1981) 1686.
- [5] E.E. Bernarducci, P.K. Bhardwaj and H.J. Schugar, *J. Am. Soc.*, 105 (1983) 3860.
- [6] I. Dudgele and J.B. Cotton *Corr. Sci.*, 3 (1963) 69.
- [7] J.B. Cotton and I.R. Scholes, *Corr. J.*, 2 (1967) 1.
- [8] R.W. Walker, *Anticorrosion* 17 (1970) 9.
- [9] G. Poling, *Corr. Sci.*, 10 (1970) 359.
- [10] S. Thiboult *Corr. Sci.*, 17 (1977) 701.
- [11] R.F. Roberts, *Electron Spectrosc. Relat. Phenom.*, 4 (1976) 273.
- [12] D. Chadwick and T.J. Electron Spectrosc. Relat. Phenom, 10 (1977) 79.
- [13] D. Chadwick and T. Hashemi *Corr. Sci.*, 18 (1978) 39.
- [14] A.R. Siedle, R.A. Velapoldi and Erickson N., *Appl. Surf. Sci.*, 3 (1979) 229.
- [15] H.G. Thompkins and S.P. Sharma, *Surf. Interf. Anal.*, 4 (1982) 261.
- [16] N.D. Hobbins and R.F. Roberts, *Surf. Technol.*, 9 (1979) 235.
- [17] D.M.L. Goodgame, M. Goodgame and M.J. Weeks *Chem. Soc. A* (1967) 1125.
- [18] M.G.B. Drew, D.H. Templeton and A. Zalkin *Inorg. Chem.*, 12 (1968) 2618.
- [19] D.P. Drolet, D.M. Manuta, A.J. Lees, A.D. Katnani and G.J. Colyle, *Inorg. Chim. Acta*, 146 (1988) 173.
- [20] R. Curini, S. Materazzi, G. D'Ascenzo and G. De Angelis *Thermochim. Acta*, 161 (1990) 297.
- [21] R. Curini, G. D'Ascenzo, S. Materazzi and A. Marino, *Thermochim. Acta*, 200 (1992) 169.
- [22] S. Materazzi, G. D'Ascenzo, R. Curini and L. Fava, *Thermochim. Acta*, 228 (1993) 197.
- [23] M. Goodgame and L.I.B. Haines, *J. Chem. Soc. A* (1966) 174.